

PYROLYSIS STUDY OF A HYDRIDE-SOL-GEL SILICA Part II. Kinetic aspects

R. Campostrini*, A. Sicurelli, M. Ischia and G. Carturan

Dipartimento di Ingegneria dei Materiali e Tecnologie Industriali, Università di Trento, via Mesiano 77, 38050 Trento, Italy

The thermal behaviour of a sol-gel prepared hydride silica gel (HSiO sample) in the 20–1000°C interval was studied by coupled thermogravimetric-mass spectrometric (TG-MS) analyses carried out at various heating rates. Thermogravimetric curve elaboration allowed the determination of the flex temperatures, corresponding to the maximum release rate of gas-evolved compounds, and to calculate the activation energy of the overall process. The mass spectrometric data, registered in the TG-MS measurements, were treated to discriminate the single reactions accounting for the release of each compound, among which water, dihydrofuran and various silane- and siloxane-derived species. These results were used to calculate the comprehensive activation energy and also those of each of the released species.

Different methods of data processing were used to achieve better reliability of calculated activation energies. The discussion focuses on the high extension of kinetic information arising from MS data processing and on the advantage of identifying the contribution of single reactions, although they occur simultaneously during the heating process. In this respect, good agreement was found between the activation energies of the overall process calculated by separately processing TG and MS data. By processing MS data, the same agreement was observed in the comparison between the activation energy calculated for the overall thermal process and in the sum of the weighed activation energies of the reaction of each released compound.

Keywords: activation energies of simultaneous thermogravimetric events, hydride silica gel, mass spectrometric analyses, pyrolysis study

Introduction

In Part 1 of this work, it was shown that HSiO-crude-gel, obtained from HSiO(CH₃)₃ hydrolysis and condensation, evolves to a SiO₂-matrix by heating up to 1000°C in inert atmosphere [1]. Pyrolysis study was carried out by working with a standard 10°C min⁻¹ heating rate. A complex pattern of pyrolysis reactions accounts for the release of gaseous silanes, siloxanes, solvent and water. These reactions were identified by TG-MS and TG-GC-MS measurements. These analyses also allowed determination of the temperature interval corresponding to each specific reaction, the trend of the release of each single species in function of temperature, and the amount of each evolved compound. This information, obtained from TG-MS measurements extended to various heating rates, is used and processed here to define the activation energies of the overall pyrolysis process and of individual reactions, with the perspective of verifying the use of mass spectrometric data as an alternative approach to ordinary TG kinetic experiments. In this respect, the case under study appears quite interesting. As a matter of fact, the complete pyrolysis of HSiO-crude-gel is a complex process, that cannot be resolved by TG measurements into defined consecutive events. The MS analysis may give sure results on the trend of each

event and on the entire process as well, so that the weight of each reaction to the activation energy of the entire transformation can be determined and discussed. With the aim of calculating more reliable values of activation energy, the TG-MS data were processed in correspondence with the highest rate of each single reaction and in correspondence with its initial step.

Experimental

Gel-sample

As reported in Part 1, the HSiO-crude-gel sample was prepared by hydrolysis and condensation of a tetrahydrofuran solution of trimethoxysilane [1]. After the gelling process, the sample was milled, dried at room temperature for 2 days and then at 80°C for 5 h. The xerogel was stored under nitrogen in a closed vessel.

Instrumentation

Thermogravimetric analyses were performed on a LabSys Setaram thermobalance operating in the 20–1000°C range, working under 100 cm³ min⁻¹ He (99.99%) flux. Thermal analyses were recorded using a constant amount of powdered sample (13.0 mg) and

* Author for correspondence: renzo.campostrini@ing.unitn.it

different heating rates: $\beta=5, 7.5, 10, 12.5, 15, 17.5$ and $20^\circ\text{C min}^{-1}$. Alumina sample holders of 0.1 cm^3 in volume were used, employing $\alpha\text{-Al}_2\text{O}_3$ as reference. Using a volume of $\alpha\text{-Al}_2\text{O}_3$ identical to the one of the used sample, a set of blank runs were performed at all the heating rates in order to correct the TG measurements for the buoyancy effect [2].

The TG-MS interface was used in all the measurements coupling the thermobalance with the TRIO 1 VG quadrupole mass spectrometer. Electron mass spectra (70 eV) were continuously recorded with frequency 1 scan s^{-1} in the 3–300 amu range. A 5 m silica capillary column (0.19 mm), thermostatted at 250°C , was used as a transfer line ensuring the mass spectrometric detection of released gas species in less than 2 s.

Results and discussion

Pyrolysis process

As described in the Part 1, the pyrolysis of the HSiO-crude-gel was studied in the $20\text{--}1000^\circ\text{C}$ interval, working with a heating rate of $10^\circ\text{C min}^{-1}$ [1]. It is described by three subsequent and partially overlapping mass losses, corresponding to:

(A) stripping of solvent molecules, entrapped in the gel network, plus dehydrogenation, i.e., dihydrofuran release

(A.1) $\text{HSiO-crude-gel} \xrightarrow{T < 300^\circ\text{C}} \text{HSiO-matrix} + \text{dihydrofuran}_{(g)}$ (gas mol%=3.1)

(B) release of water (bimodal trend) by condensation of residual silanol groups along the siloxane chains

(B.1) $2\equiv\text{Si-OH} \xrightarrow{T \text{ around } 240 \text{ and } 470^\circ\text{C}} \equiv\text{Si-O-Si}\equiv\text{matrix} + \text{H}_2\text{O}_{(g)}$ (gas mol%=3.9)

(C) evolution of silanes and siloxane oligomers by $\equiv\text{Si-H}/\equiv\text{Si-O}$ bond exchanges among the siloxane chains (where silane and disiloxane constitute the main mass loss) yielding a relevant gel skeleton rearrangement

(C.1) $\text{HSiO-crude-gel} \xrightarrow[T \text{ around } 400^\circ\text{C}]{3\equiv\text{Si-H}/\equiv\text{Si-O bond exch.}} \text{SiO}_2\text{-matrix} + \text{SiH}_4_{(g)}$ (gas mol%=78.3)

(C.2) $\text{HSiO-crude-gel} \xrightarrow[T \text{ around } 400^\circ\text{C}]{2\equiv\text{Si-H}/\equiv\text{Si-O bond exch.}} \text{SiO}_2\text{-matrix} + \text{H}_3\text{SiOCH}_3_{(g)}$ (gas mol%=2.2)

(C.3) $\text{HSiO-crude-gel} \xrightarrow[T \text{ around } 400^\circ\text{C}]{4\equiv\text{Si-H}/\equiv\text{Si-O bond exch.}} \text{SiO}_2\text{-matrix} + \text{H}_3\text{SiOSiH}_3_{(g)}$ (gas mol%=12.1)

(C.4) $\text{HSiO-crude-gel} \xrightarrow[T \text{ around } 400^\circ\text{C}]{5\equiv\text{Si-H}/\equiv\text{Si-O bond exch.}} \text{SiO}_2\text{-matrix} + \text{H}_3\text{SiOSi(H)}_2\text{OSiH}_3_{(g)}$ (gas mol%=0.4)

TG-MS measurements and kinetic treatment of TG data

The trends and the relative intensities of the (A), (B) and (C) thermogravimetric events resulted unchanged for the HSiO-gel sample in the TG-MS measurements recorded at the various heating rates, as shown in the TIC curves, plotted vs. time, of Fig. 1. The rate increase only yields a progressive shift of the TIC peaks. This trend is not evident in the case of a direct comparison of the TG curves, because the buoyancy effect deeply modifies the shape of these curves even after correction with their respective blank measurements. Therefore, the experimental values in the central part of the TG curves, registered at the various temperatures, were interpolated by different kinds of mathematic functions. In this data processing, the points corresponding to a ca. 200°C interval were considered for each TG curve. The best interpolations were obtained by considering 8th degree polynomial functions, reported in Fig. 2, chosen on the basis of their correlation coefficient (R^2) values calculated by least square method. The plots of the derivates of these polynomial functions allowed determination of the flex point temperatures (T_{flex}), reported in Table 1 together with R^2 values.

The Flynn–Wall–Ozawa (FWO) method [3–5] was used to calculate the Arrhenius parameters [6], according to the equation:

$$\lg \beta = \lg \frac{AE^\ddagger}{RF(\alpha)} - 2.315 - 0.4567 \frac{E^\ddagger}{RT}$$

where β is the linear heating rate, A the pre-exponential factor, E^\ddagger the activation energy, R the gas constant, $F(\alpha)$ the integral mechanism function and T the absolute temperature [7–10]. In this TG data processing, T_{flex} temperature values were used. The Arrhenius plot of the log heating rate vs. the inverse of these constant conversion T_{flex} temperatures is shown in Fig. 3. With this procedure, an activation

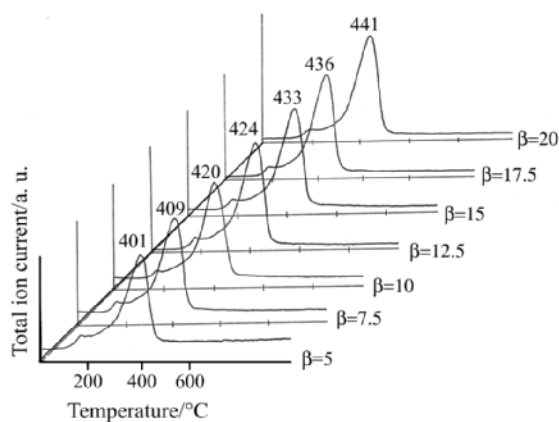


Fig. 1 TG-MS analyses of HSiO-gel sample carried out at different heating rates (β from 5 to $20^\circ\text{C min}^{-1}$): total ion current curve of the evolved gas species vs. pyrolysis temperature

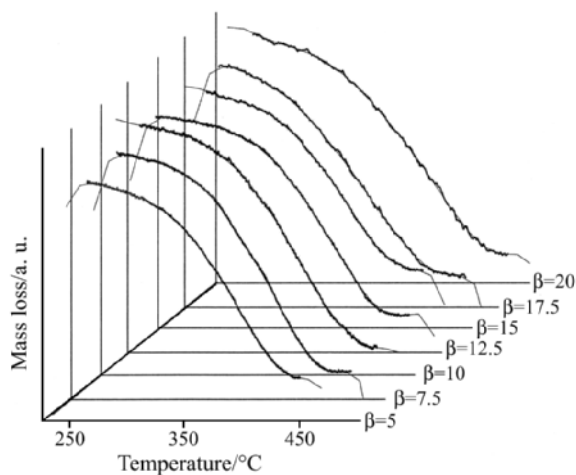


Fig. 2 Thermogravimetric measurements of an HSiO-gel sample. Central part of the TG curves, carried out at the various heating rates, interpolated by 8th degree polynomial functions

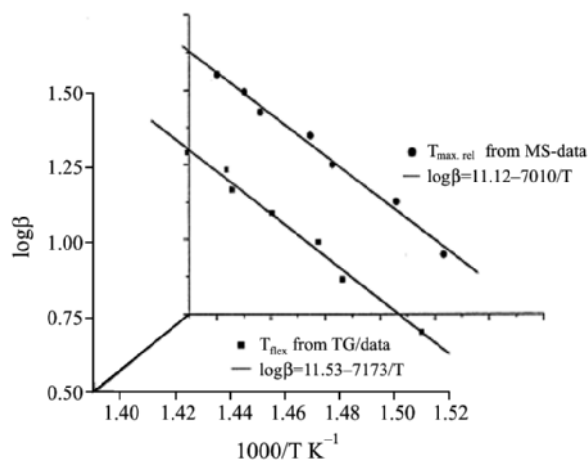


Fig. 3 Arrhenius plot of heating rate–temperature of constant conversion data, referring to the total pyrolysis process of HSiO-gel, calculated from TG-data (T_{flex}) and MS-data ($T_{\text{max,rel}}$)

energy of $31.2 \pm 1.6 \text{ kcal mol}^{-1}$ was calculated, referring to the total pyrolysis process.

The approach used here and the calculated E^\ddagger value deserve further comment. Indeed, the choice of the flex point temperature, when the mass loss reaction is fastest, would be avoided for kinetic reasons [11, 12]. On the other hand, the uncertain trends of the first part of these TG curves, due to the buoyancy effects, do not allow correct comparison of temperatures corresponding to lower constant conversions (for instance, conversion values of $\alpha=0.1$). Nevertheless, the progressive mass loss of the HSiO-crude-gel refers to the (A), (B) and (C) overlapping processes where network rearrangements due to the $\equiv\text{Si-H}/\equiv\text{Si-O}$ bond exchanges (reactions (C.1)–(C.4)) are dominant around 400°C . Although four species were simultaneously released around this temperature,

Table 1 Thermogravimetric data. Flex temperatures calculated from the plots of the derivatives of the 8th degree polynomial functions, which better interpolate the central points (ca. 200°C temperature range) of the thermogravimetric curves (corrected by the buoyancy effect), in function of the various heating rates

$\beta/$ $^\circ\text{C min}^{-1}$	Correlation coefficient (R^2) of the 8 th degree polynomial function	Flex temperature/ $^\circ\text{C}$
5	0.9999	389
7.5	0.9998	402
10	0.9998	406
12.5	0.9999	414
15	0.9998	421
17.5	0.9998	422
20	0.9996	429

β – heating rate

these compounds are formed by the same type of reaction mechanism. Moreover, temperatures of the earlier step of the sample mass loss (low conversion) also correspond to the release of species generated by different chemical mechanisms (i.e., the stripping of solvent and the water release by silanol condensation), which play a minor role in total mass loss. These issues prompted us to select temperatures corresponding to the highest rate of the mass loss. Consequently, calculated $E^\ddagger=31.2 \pm 1.6 \text{ kcal mol}^{-1}$ is not associated with a single chemical reaction, but to the sum of the (A), (B) and (C) processes [13].

Kinetic treatment of MS data

Kinetic results from TG curves revealed an interesting counterpart through the treatment of mass spectrometric data. In TG-MS measurements, the TIC curve detects the evolution of all the species released during the sample mass loss. The temperature of the maximum of the TIC peak indicates the maximum gas phase release ($T_{\text{max,rel}}$) corresponding to the highest rate of the reactions occurring in the solid sample. Table 2 reports these $T_{\text{max,rel}}$ temperatures determined in the TG-MS measurements carried out at the various heating rates. Analogously to treatment of TG data, these TIC peak temperatures were used to plot the Arrhenius graph reported in Fig. 3. The activation energy obtained was $E^\ddagger=30.5 \pm 1.4 \text{ kcal mol}^{-1}$, i.e., very close to $E^\ddagger=31.2 \pm 1.6 \text{ kcal mol}^{-1}$ found by TG data processing. This fact supports the approach used to calculate the activation energy from the MS data in alternative to the TG data.

Actually, information resulting from MS data presents a much higher qualification with respect to TG analysis. In fact, the trend of the TG curve does not allow separation of the contributions of single mass losses when the whole thermogravimetric event is due

Table 2 Mass spectrometric data from TG-MS measurements. Temperatures corresponding to: (a) the maximum of the TIC peak or the maximum of the single m/z ion current peak (maximum release) of the representative ions, in function of the pyrolysis heating rate; (b) the 10% of the total area of these peaks (10% release)

Chemical species	m/z signal (represent. ion)	Temperature, (a) and (b) case/ $^{\circ}\text{C}$	Heating rate of the TG-MS analyses/ $^{\circ}\text{C min}^{-1}$						
			5	7.5	10	12.5	15	17.5	20
All	TIC	(a) max release	401	409	420	424	433	436	441
		(b) 10% release	238	247	266	270	282	294	298
H_2O	18	(a) max release	216	224	237	243	252	259	270
		(b) 10% release	143	142	157	159	169	188	190
Dihydrofuran	70	(a) max release	156	164	171	177	185	186	192
		(b) 10% release	134	146	151	159	165	171	172
SiH_4	31	(a) max release	404	414	424	426	435	438	444
		(b) 10% release	281	293	302	309	315	322	327
H_3SiOCH_3	61	(a) max release	378	386	405	402	426	431	450
		(b) 10% release	297	306	312	322	331	333	339
$\text{H}_3\text{SiOSiH}_3$	77	(a) max release	384	389	403	405	411	413	416
		(b) 10% release	297	310	318	325	334	337	343
$\text{H}_3\text{SiOSi(H)}_2\text{OSiH}_3$	123	(a) max release	378	383	398	404	409	410	417
		(b) 10% release	324	330	331	344	351	354	361

Table 3 Arrhenius graphs from TG-MS measurements. Straight lines obtained by considering data ($\log\beta$ vs. $1/T$) listed in Table 2. Temperature values correspond to: (a) the maximum of the TIC peak or to the maximum of the single m/z ion current peak (maximum release) of the representative ions, in function of the heating rate; (b) the same for the temperatures corresponding to the 10% of the total area of these peaks (10% release); (c) comparison with flex point temperatures calculated from TG curves

Chemical species	m/z signal (represent. ion)	Temperature of (a), (b) and (c) case/ $^{\circ}\text{C}$	Arrhenius straight line: $y=ax+b$ and (R) values			
			a	b	(R)	$\Delta E^{\ddagger}/\text{kcal mol}^{-1}$
All	TIC	(a) max release	-7010 ± 322	11.12 ± 0.46	0.9948	30.5 ± 1.4
		(b) 10% release	-2733 ± 188	6.09 ± 0.34	0.9884	11.9 ± 0.8
H_2O	18	(a) max release	-2930 ± 210	6.74 ± 0.41	0.9874	12.7 ± 0.9
		(b) 10% release	-1989 ± 322	5.61 ± 0.74	0.9403	8.7 ± 1.4
Dihydrofuran	70	(a) max release	-3280 ± 152	8.37 ± 0.34	0.9946	14.3 ± 0.7
		(b) 10% release	-2730 ± 110	7.51 ± 0.26	0.9961	12.1 ± 0.5
SiH_4	31	(a) max release	-7366 ± 355	11.59 ± 0.51	0.9942	32.0 ± 1.5
		(b) 10% release	-4370 ± 86	8.59 ± 0.15	0.9990	19.0 ± 0.4
H_3SiOCH_3	61	(a) max release	-3552 ± 555	6.27 ± 0.82	0.9440	15.5 ± 2.4
		(b) 10% release	-4771 ± 294	9.10 ± 0.50	0.9906	20.8 ± 1.3
$\text{H}_3\text{SiOSiH}_3$	77	(a) max release	-7798 ± 641	12.59 ± 0.95	0.9835	33.9 ± 2.8
		(b) 10% release	-4613 ± 120	8.79 ± 0.20	0.9983	20.1 ± 0.5
$\text{H}_3\text{SiOSi(H)}_2\text{OSiH}_3$	123	(a) max release	-6501 ± 526	10.72 ± 0.78	0.9840	28.3 ± 2.3
		(b) 10% release	-5557 ± 697	10.09 ± 1.13	0.9628	24.2 ± 3.0
All	TG data	(c) flex point	-7173 ± 368	11.53 ± 0.54	0.9930	31.2 ± 1.6

to the contribution of multiple simultaneous chemical reactions. This same feature is also common to the trend of the TIC curve, that is formed by the sum of all the fragmentation ions of all the released species. Nevertheless, from the TG-MS data, the contribution of single m/z ion currents can be easily extrapolated. These m/z signals, if appropriately selected, can monitor the evolution of single compounds formed by specific chemical reactions independently of the simultaneous occurrence of the other reactions.

The ion currents of the representative ions ($m/z(i^*)$) of each detected compound (Part 1, pyrolysis process, qualitative description) were plotted for the TG-MS measurements recorded at the various heating

rates. The temperatures corresponding to the maximum peak of each m/z ion current are reported in Table 2. These temperatures correspond to the maximum rate of the release of each species ($T_{\text{max rel.}}$) resulting from a definite chemical reaction. The $T_{\text{max rel.}}$ values were used to plot the Arrhenius graph of each reaction (FWO equation). Table 3 reports the parameters used to calculate the activation energies of each reaction. It is noteworthy that the activation energy of the entire pyrolysis process (previously calculated from the maximum of TIC curves, $30.5\pm 1.4 \text{ kcal mol}^{-1}$) agrees with the value obtained from the 'weighed sum' of the activation energies of each single reaction: i.e., $\sum E_j^{\ddagger} \chi_j =$

$30.5 \pm 1.6 \text{ kcal mol}^{-1}$; where χ_j is the molar fraction that each compound (yielded from its specific reaction) presents in the gas phase throughout pyrolysis (Part 1, Table 2, $\chi_j = \text{mol}\%/100$). This fact may not be trivial. As a general working procedure, activation energy of a complex thermal process (i.e., multiple reactions occurrence) is currently reported without any specification of the individual contributions. Thus, a value so calculated might be related to the major chemical reaction alone, or to the more energy demanding event, or the weighed sum of each reaction. This latter possibility is demonstrated by our data. It is based on the very similar values found for the activation energies calculated from T_{flex} temperatures of TG data, from the $T_{\text{max rel.}}$ temperatures of TIC curves, and from the weighed sum of E^\ddagger values obtained from the $T_{\text{max rel.}}$ temperatures of the $m/z(i^*)$ ion current curves of each evolved compound.

As a general observation, appropriate kinetic treatment of experimental data requires calculation of the reaction rate from its initial steps and not from its maximum course [11, 14]. Consequently, for each compound, the temperature corresponding to an arbitrary constant conversion of 10% (with respect to its total evolved amount during the entire pyrolysis process) was chosen to more appropriately calculate the Arrhenius plot. For each $m/z(i^*)$ ion current curve, the temperature corresponding to 10% of the total integrated area was determined ($T_{10\%A}$). These $T_{10\%A}$ temperatures are reported in Table 2. From these data, new activation energy values were calculated, as reported in Table 3. These new E^\ddagger values appear more coherent and homogeneously subdivided, taking into account the different (A), (B) and (C) processes which characterize the pyrolysis behaviour of the HSiO-crude-gel sample. The activation energies, calculated from $T_{10\%A}$ temperatures, were:

- Stripping and dehydrogenation of solvent molecules (release of dihydrofuran, A.1), $E^\ddagger = 12.1 \pm 0.5 \text{ kcal mol}^{-1}$.
- Condensation of silanol groups (release of water, B.1), $E^\ddagger = 8.7 \pm 1.4 \text{ kcal mol}^{-1}$.
- Siloxane chain rearrangements due to $\equiv\text{Si-H}/\equiv\text{Si-O}$ bond exchanges (release of silane monomers and siloxane oligomers, C.1–C.4), E^\ddagger from 19.0 ± 0.4 to $24.2 \pm 3.0 \text{ kcal mol}^{-1}$.

These data are conceivable, considering that: (i) silane and siloxane species release requires the same kind of Si–H and Si–O bond cleavage, and must involve the same approach of a relevant number of HSi–(O)₃ units locking together in the transition state. This fact may require a very high activation entropy demand, justifying the $E^\ddagger = 19.0$ – $24.2 \text{ kcal mol}^{-1}$ values; (ii) solvent stripping may be considered a diffusive process that requires a lower activation energy

than other chemical reactions, whereas dehydrogenation process may be supported and favoured by a catalytic interaction between the solvent molecule and the hydride-functionalised HSiO-matrix; (iii) water release may be facilitated by the high mobility of H⁺ species, which is recognized as an active catalyst in Si–OH vs. Si–OH condensation [15].

An additional element of discussion may be derived from the activation energy of the whole pyrolysis process, which is calculated by considering the $T_{10\%A}$ temperatures of the total integrated TIC curves. In this case, a $E^\ddagger = 11.9 \pm 0.8 \text{ kcal mol}^{-1}$ is calculated in disagreement with values found for the release of SiH₄ ($E^\ddagger = 19.0 \pm 0.4 \text{ kcal mol}^{-1}$) and H₃SiOSiH₃ ($E^\ddagger = 20.1 \pm 0.5 \text{ kcal mol}^{-1}$) species, which constitute the main mass loss event. Actually, the $T_{10\%A}$ temperatures determined for the TIC curves fell in the temperature range corresponding to the early stage of the pyrolysis, where the condensation and the stripping (+dehydrogenation) reactions are dominant. In fact, if the release of the silane-derived species is neglected in this temperature range and only the amounts of water and dihydrofuran are considered, the nominal composition of the released phase becomes: H₂O, 55.1 mol%; dihydrofuran, 44.9 mol%. Consequently, a molar average value of the weighed activation energy $\sum_{\text{water}}^{\text{solvent}} E_j^\ddagger \chi_j = 10.2 \pm 1.0 \text{ kcal mol}^{-1}$ can be calculated. This value agrees with the $E^\ddagger = 11.9 \pm 0.8 \text{ kcal mol}^{-1}$ previously determined using the $T_{10\%A}$ temperatures of the TIC curves. On the other hand, taking into account the more accurate activated energy values obtained from the $T_{10\%A}$ temperatures of each released compounds and their molar percentages in the gas phase evolved during the whole pyrolysis process, a nominal activation energy of $\sum E_j^\ddagger \chi_j = 18.6 \pm 0.5 \text{ kcal mol}^{-1}$ was calculated for the total process. This last nominal value agrees with the activation energy found for the silane release ($E^\ddagger = 19.0 \pm 1.4 \text{ kcal mol}^{-1}$), which is the main component detected in the evolved gas phase (78 mol%).

In conclusion, this work demonstrates that the kinetic study of complex thermal phenomena occurring in the solid state can be performed by mass-spectrometric analysis of gas-released species, by considering the temperature of the TIC maximum as equivalent to the flex temperature in TG experiments. Moreover, the possibility that MS analysis offers for isolating the ion current curve of each gas species allows the calculation of the activation energy of individual chemical reactions even if they occur simultaneously. In this respect, the activation energy of the entire process (calculated by different approaches) has been found equivalent to the sum of the weighed contribution of the intrinsic activation energies of each reaction.

Conclusions

The pyrolysis of the hydride-functionalized sol-gel silica HSiO-sample was described by three subsequent and partially overlapping thermogravimetric events. The complex pattern of reactions occurring in the solid during heating was defined by identifying the compounds released in gas phase by means of coupled TG-MS and TG-GC-MS analyses. The reaction mechanisms involved: (A) release of dihydrofuran by stripping of solvent molecules entrapped in the gel network (reaction (A.1)); (B) release of water by condensation of residual silanol groups present along the siloxane chains (reaction (B.1)); (C) release of silane monomers and siloxane oligomers by $\equiv\text{Si-H}/\equiv\text{Si-O}$ bond exchanges inside the gel skeleton (reactions (C.1)–(C.4)).

In this contribution, kinetic aspects concerning the occurrence of these reactions were investigated by TG-MS measurements carried out at various heating rates ($5\text{--}20^\circ\text{C min}^{-1}$). The Flynn–Wall–Ozawa method was used to determine Arrhenius parameters leading to activation energy values. Both TG- and MS-data were treated separately in order to calculate an activation energy value attributable to the entire pyrolysis process. The value $E^\ddagger=31.2\pm 1.6\text{ kcal mol}^{-1}$ was obtained from TG data by considering the flex temperatures of the TG curves, whereas $E^\ddagger=30.5\pm 1.4\text{ kcal mol}^{-1}$ was obtained from MS data by considering the maximum TIC peak temperatures. The good correlation demonstrates the validity of this new approach of the MS data processing as an alternative to the TG data elaboration. The evolution of each released compound was monitored by plotting the $m/z(i^*)$ ion curve of its representative ion, independently of the occurrence of the other reactions. By considering the maximum peak temperatures of these representative ions, the activation energies of each single reaction (A.1), (B.1), (C.1)–(C.4) were determined. The sum of these activation energies, multiplied by the molar fraction that the yielded compound had in the total evolved gas phase, led to a weighed average activation energy value of $\sum E_j^\ddagger \chi_j = 30.5\pm 1.6\text{ kcal mol}^{-1}$. This fact demonstrates that, in general working procedure, the common activation energy value (calculated from temperatures corresponding to high conversion degrees) attributed to the entire pyrolysis process (when consisting of several overlapping thermogravimetric events) can be associated with the weighed sum of the activation energy values of the simultaneously occurring reactions in the same mass loss. As required for appropriate kinetic data processing, temperatures corresponding to a lower conversion degree were successively selected in order to calculate more accurate activation energy values. Temperatures corresponding to a constant conversion

of 10% (with respect to the total evolved amount of each compound) were determined from the integrated area of each representative m/z ion current. These new activation energy values, although quite different from the previous ones, were more coherent in view of the different kind of reaction mechanisms involved in the pyrolysis of this HSiO-gel: stripping+dehydrogenation of solvent, $E^\ddagger=12.1\pm 0.5\text{ kcal mol}^{-1}$; silanol group condensation, $E^\ddagger=8.7\pm 1.4\text{ kcal mol}^{-1}$; siloxane chain rearrangements by $\equiv\text{Si-H}/\equiv\text{Si-O}$ bond exchanges, E^\ddagger from 19.0 ± 1.4 to $24.2\pm 3.0\text{ kcal mol}^{-1}$.

Acknowledgements

We would like to thank Dr. Brian Martin for the revision to the English.

References

- 1 R. Camprostrini, A. Sicurelli, M. Ischia and G. Cartuan, *J. Therm. Anal. Cal.*, OnlineFirst, DOI: 10.1007/s10973-006-7623-1.
- 2 P. J. Haines, *Principles of Thermal Analysis and Calorimetry*, RSC Paperbacks, Cambridge, UK 2002.
- 3 T. Ozawa, *Bull. Chem. Soc. Jpn.*, 38 (1965) 1881.
- 4 J. H. Flynn and L. A. Wall, *Polym. Lett.*, 4 (1966) 323.
- 5 T. Ozawa, *Thermochim. Acta*, 203 (1992) 159.
- 6 ASTM International E 1641-04. Standard Test Method for Decomposition Kinetics by Thermogravimetry, 100 Barr Harbor Drive, PO Box C700, West Conshohocken, PA 19428-2959 US.
- 7 Y. Pan, X. Guan, Z. Feng, Y. Wu and X. Li, *J. Therm. Anal. Cal.*, 55 (1999) 877.
- 8 C. A. Ribeiro, M. S. Crespi, C. T. R. Guerriero and A. M. Veronezi, *Eclat. Quim.*, 26 (2001) 185.
- 9 J. G. Santos, M. M. Conceicao, M. F. S. Trindade, A. S. Araujo, V. J. Fernandes Jr. and A. G. Souza, *J. Therm. Anal. Cal.*, 75 (2004) 591.
- 10 J. J. Zhang and N. Ren, *J. Chem.*, 22 (2004) 1459.
- 11 W. C. Gardiner Jr., *Rates and Mechanisms of Chemical Reactions*, Ed. W. A. Benjamin, Inc. New York, USA 1969.
- 12 Z. R. Lu, Y. C. Ding, Y. Xu, Q. Liu and J. P. Lang, *Chin. J. Chem.*, 22 (2004) 1091.
- 13 K. S. Khairou, *J. Therm. Anal. Cal.*, 69 (2002) 583.
- 14 T. P. Prasad, S. B. Kanungo and H. S. Ray, *Thermochim. Acta*, 203 (1992) 503.
- 15 C. J. Brincker and G. W. Scherer, *Sol-Gel Science: The Physics and Chemistry of Sol-Gel Processing*, Ed. Academic Press, San Diego CA 1990.

Received: April 12, 2006

Accepted: July 20, 2006

OnlineFirst: February 13, 2007

DOI: 10.1007/s10973-006-7624-0